that all field components are multiplied by $\exp(j\omega t)$ for harmonic excitation. The above field expressions convert into the well-known fields of the shielded line without dielectric [4], [7], [8] for $\epsilon_2' = 1$.

References

[1] W. Meyer, "Dielectric measurements on polymeric materials by using superconducting microwave resonators," *IEEE Trans. Microwave Theory Tech.*, vol. 25, pp. 1092–1099, 1977.

[2] H. Kaden, "Eine allgemeine Theorie des Wendelleiters," *Arch. Elek. Übertragung.*, vol. AEÜ-5, pp. 534–538, 1951.

[3] W. Sichak, "Coaxial line with helical inner conductor," *Proc. IRE*, pp. 1315–1319, 1953.

[4] W. Pöschl, "Wellenfortpflanzung längs einer Wendel mit zylindrischem Aussenleiter," *Arch. Elek. Übertragung.*, vol. AEÜ-7, pp. 518–522, 1953.

[5] G. Piefke, "Reflexion in Wendelleitungen bei Änderung der Wendelsteigung," *Arch. Elek. Übertragung.* vol. AEÜ-9, pp. 369–374, 1955.

[6] L. Stark, "Lower modes of a concentric line having a helical inner conductor," *J. Appl. Phys.*, vol. 25, pp. 1155–1162, 1954.

[7] J. H. Bryant, "Some wave properties of helical conductors," *Electr. Commun.*, vol. 31, pp. 50–56, 1954.

[8] D. J. Miley, "Field analysis of helical resonators with constant-bandwidth filter application," *IEEE Trans. Parts, Mater., Packag.*, vol. PMP-5, pp. 127–128, 1969.

[9] G Rotter, "Die Berechnung der Kenngrössen von Wendelleitungs-resonatoren," *Arch. Elek. Übertragung.*, vol. AEÜ-25, pp. 25–31, 1971.

[10] R. A. Waldron, "Perturbation theory of resonant cavities," *Proc. Inst. Elec. Eng.*, pp. 272–274, 1960.

[11] F. Horner *et al.*, "Resonance methods of dielectric measurements at centimetre wavelength," *Proc. Inst. Elec. Eng.*, vol. 89, pt. III, pp. 53–68, 1946.

[12] P. Kneisel *et al.*, "Nb_3Sn for superconducting RF-activities," *Adv. Cryogenic Eng.*, vol. 22, pp. 341–346, 1977.

[13] P. Kneisel *et al.*, "Properties of superconducting Nb_3Sn for hf-cavities," in *Proc. 1977 int. Cryogenic Materials Conf.*, (Boulder, CO), Aug. 2–5, 1977.

[14] E. Voges and V. K. Petermann, "Losses in superconducting coaxial transmission lines," *Arch. Elek. Übertragung.*, vol. AEÜ-27, pp. 384–388, 1973.

[15] J. Halbritter, "On interfacial tunneling of superconducting surfaces," *Phys. Lett.*, vol. 43A, pp. 309–310, 1973.

[16] J. Halbritter, "On rf-residual losses and phonon generation," *IEEE Trans. Magn.*, vol. MAG-II, pp. 427–430, 1975.

[17] W. Meyer, "High sensitivity dielectric loss measurements by using superconducting microwave resonators in an oscillator loop," *Electron. Lett.* vol. 13, pp. 7–8, 1977.

[18] W. Meyer, "New materials for superconductive communication cables," *IEEE Trans. Commun.*, vol. 25, pp. 449–458, 1978.

[19] J. le G. Gilchrist and W. Meyer, "Dielectric loss spectrum of hydrated vitreous silica," in *Advances in Cryogenic Engineering* vol. 24, K. D. Timmerhaus *et al.*, Eds. New York: Plenum, 1978.

[20] W. Meyer, "Variation of dielectric microwave losses in PE as the result of different sample treatments," in *Nonmetallic Materials and Composites at Low Temperatures*, A. F. Clark *et al.*, Eds. New York: Plenum, 1979.

[21] A. Kraszewski, "Microwave instrumentation for moisture content measurement," *J. Microwave Power*, vol. 8, pp. 323–335, 1973.

[22] W. Meyer and W. Schilz, "Microwave absorption by water in organic materials," *Dielectric Materials, Measurements and Applications* Inst. Elec. Eng. Publ. 177, 1979, pp. 215–219.

Measurement of Losses in Noise-Matching Networks

ERIC W. STRID

***Abstract*—The noise contribution of an input-matching network to a low-noise amplifier is equal to the inverse of the network's available gain. The available gain of various networks at 4 GHz was computed from high-accuracy *S*-parameter measurements. The available gain of a typical tuner was experimentally found to be a strong function of its tuning, which shows that "back-to-back" measurements of two tuners to obtain the loss of each tuner can be inaccurate. Measurement of the available gain of an amplifier's input-matching circuit is shown to give quick insight into its minimum noise contribution before the actual amplifier stage is built.**

I. Introduction

SOME APPLICATIONS of microwave amplifiers require squeezing out every bit of low-noise performance from an active device. One such application is a satellite earth station low-noise amplifier, whose contribution to system operating noise temperature is relatively large due to the low equivalent temperature of the antenna [1]. Development of such amplifiers requires selection of the best active devices, circuit materials, and techniques.

The noise of active two-ports is usually characterized with an impedance-substitution setup such as that shown in Fig. 1 [2]. Small losses in the components between the noise generator and the device under test (DUT) contribute directly to the total noise figure, and the accuracy to which this loss is known contributes directly to the accuracy of the noise-figure measurement. In current practice, the losses of typical input circuits used in microwave-transistor noise-test setups are in the range of 0.1–1 dB. This range is normally much greater than the uncertainty in the calibration of the noise source. Because this uncertainty leads to inaccurate noise data for the device, especially $F_{\min}$ data,

Manuscript received June 3, 1980; revised October 28, 1980.

The author was with Farinon Transmission Systems, San Carlos, CA. He is now with Applied Research Group, Tektronix Laboratories, Tektronix, Inc., Beaverton, OR 97077.

0018-9480/81/0300-0247$00.75

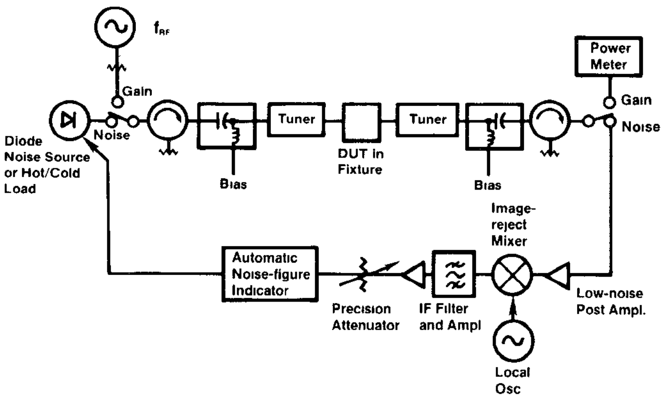

Fig. 1. Microwave transistor noise characterization system [2].

an amplifier stage designed with the rough data must sometimes be built before the full capabilities of the device are known. Such cut-and-try techniques are very inefficient.

Although the input noise-matching networks of low-noise amplifiers are selected on the basis of their relative noise-figure performances, the absolute losses of these networks are usually not known. Transistor chips used in such an amplifier normally cannot be removed for testing or for performance comparisons in another circuit. To compare circuits, several amplifiers must be made with chips from the same lot in order to obtain a statistical sample of circuit performance. This procedure is very tedious and inefficient, especially when the best devices available are used.

In the following section, the appropriate loss of a noise-matching network is discussed. Various methods of measuring these losses are thus examined, including the popular "back-to-back" method. The assumptions inherent in the back-to-back method are shown to be poor, but the direct measurement of the network S-parameters with sufficient accuracy is shown to lead to useful loss data. The loss of a typical slide-screw tuner is shown to be a strong function of the magnitude and angle settings, and the losses of input circuits for a 4-GHz low-noise amplifier are shown.

II. Loss in the Matching Network

Fig. 2 shows the block diagram of the circuit elements for a low-noise input stage. Network M in Fig. 2 refers to the following components of Fig. 1: switch, isolator, bias network, input tuner, and any adaptors and/or cables between the noise generator and the DUT. For an amplifier stage, network M consists of all the components that are used to effect a noise match between the input and the first-stage transistor and to provide any necessary bias. In Fig. 2, S_{ij} refers to the S-parameters of network M, Γ_g is the reflection coefficient of the noise generator (or input termination), and Γ_2 is the reflection coefficient "looking into" network M from the active device. The characteristic impedances of the networks are assumed to be equal, so no

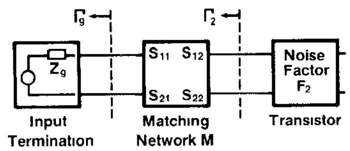

Fig. 2. Block diagram of a low-noise input match.

Z_0 normalization factors are included in the following equations.

The noise factor F (noise figure = noise factor expressed in decibels) of a cascade of noisy two-ports [3] is given by

$$F=F_1+\frac{F_2-1}{G_1}+\frac{F_3-1}{G_1G_2}+\cdots \tag{1}$$

where F_n and G_n are the noise factor and the available gain, respectively, of the nth two-port. The available gain of a two-port is the ratio of its available output power to the power available from its input source. The available gain α of a passive two-port is less than 1, and its noise factor is the factor by which available power is attenuated in passing through it, i.e., $1/\alpha$ [4]. Thus, the noise factor of the cascade of a passive two-port and a two-port with noise factor F_2 is simply F_2/α.

For network M in Fig. 2, the available gain is [5]

$$\alpha=\frac{|S_{21}|^2(1-|\Gamma_g|^2)}{(1-|\Gamma_2|^2)|1-S_{11}\Gamma_g|^2} \tag{2}$$

where

$$\Gamma_2=S_{22}+\frac{S_{21}S_{12}\Gamma_g}{1-S_{11}\Gamma_g}. \tag{3}$$

Thus, the noise contribution of a passive network depends on its source immittance but is independent of its load immittance. It should be noted that this is different than a two-port's power gain or transducer gain.

The noise factor of the two-port F_2 (in this case, a transistor) has the familiar dependence [4] on the source reflection coefficient Γ_2

$$F_2=F_{\min}+\frac{r_n}{\mathrm{Re}(Y_2)}|Y_2-Y_{\min}|^2 \tag{4}$$

$$=F_{\min}+4r_n\frac{|\Gamma_2-\Gamma_{\min}|^2}{(1-|\Gamma_2|^2)|1+\Gamma_{\min}|^2} \tag{5}$$

where $F_{\min}$ = transistor's optimum noise factor, r_n = transistor's noise resistance, $Y_{\min}$ = transistor's optimum source admittance, corresponding to $\Gamma_{\min}$, and Y_2 = source admittance, corresponding to Γ_2.

For calculation of the cascaded noise figure given in (1), the available gain of the first stage G_1 must be known and is also dependent on its source reflection coefficient Γ_2. In practice, the gain measurement is simplified by measuring both the gain and the noise figure with an isolator after the stage(s) under test, as in Fig. 1. This isolator effectively makes the (measured) power gain equal to the (desired) available power gain, regardless of how the DUT's input and output tuners are adjusted.

For the case of an ideal generator impedance $\Gamma_g = 0$, the available gain simplifies to

$$\alpha_0 = \frac{|S_{21}|^2}{1-|S_{22}|^2} \tag{6}$$

where the subscript 0 denotes $\Gamma_g = 0$.

The assumption of ideal generator impedance leads to some error, even with relatively small $|\Gamma_g|$. Equations (2) and (3) can be rearranged to give

$$\alpha = \frac{|S_{21}|^2(1-|\Gamma_g|^2)}{(1-|S_{22}|^2)+|\Gamma_g|^2(|S_{11}|^2-|D|^2)-2\,\mathrm{Re}(\Gamma_g M)} \tag{7}$$

where

$$D = S_{11}S_{22} - S_{21}S_{12}$$

and

$$M = S_{11} - DS_{22}^*.$$

For $|\Gamma_g| \ll 1$, the first order effect is from the denominator

$$\alpha \simeq \frac{\alpha_0}{1-2\dfrac{\mathrm{Re}(\Gamma_g M)}{1-|S_{22}|^2}} \tag{8}$$

and α ranges from α_{min} to α_{max}, depending on the relative phase of Γ_g and M

$$\alpha_{\substack{min\\max}} \simeq \frac{\alpha_0}{1 \pm 2|\Gamma_g|\left|S_{11}+\alpha_0 S_{22}^* \dfrac{S_{12}}{S_{21}^*}\right|}. \tag{9}$$

Here, α would seem to have a very large Γ_g dependence, but as M approaches a lossless network, [6] the factor multiplying $|\Gamma_g|$ approaches 0 and α_0, α_{min}, and α_{max} all approach unity. For a typical case of the tuner discussed in the following, if $|\Gamma_g| = 0.05$ and $\alpha_0 = -0.55$ dB, then $\alpha_{min} = -0.58$ dB and $\alpha_{max} = -0.52$ dB.

The available and the delivered powers have also been discussed for the cases of different ambient temperatures, [3], [7] for multiports, [8] and for n-cascaded two-ports [9]. Other sources of noise-measurement error, including noise-source calibration and mismatch, Y-factor accuracy, second-stage noise contribution, ambient-temperature corrections, etc., are also very important to the noise measurement, but are beyond the scope of this discussion.

III. Tuner Loss Experiments

Probably the most popular method of measuring what is loosely called "tuner loss" is to lock the tuner at its setting, then to cascade it with another tuner of the same type that is tuned to conjugate match the first tuner, and finally, to measure the substitution loss [6] of the cascade in a 50-Ω (or Z_0) system. The second tuner matches the S_{22} of the first tuner back to Z_0, and the assumption is that half of the measured loss was caused by each tuner, since they are similarly constructed.

Two tuners shown thus connected in Fig. 3 have S-parameters S_{ija} and S_{ijb} with port 2 of tuner a connected to port 1 of tuner b. The transmission of the cascade is

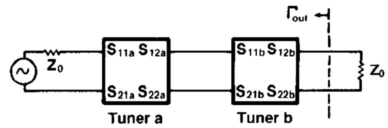

Fig. 3. "Back-to-back" measurement of tuners.

$$S_{21tot} = \frac{S_{21a}S_{21b}}{1-S_{22a}S_{11b}}. \tag{10}$$

We seek the necessary conditions on $[S_a]$ and $[S_b]$ for the available gain of the first tuner with ideal source impedance to be equal to half of this attenuation

$$\frac{|S_{21a}|^2}{1-|S_{22a}|^2} = |S_{21tot}|. \tag{11}$$

An illustrative sufficient condition is

$$S_{11b} = S_{22a}^* \tag{12a}$$

$$|S_{21a}| = |S_{21b}|. \tag{12b}$$

That is, if tuner b is adjusted so that its S_{11} is the conjugate of tuner a's S_{22} and simultaneously has the same $|S_{21}|$, then the attenuation of the cascade is indeed twice the available gain (in decibels) of tuner a at that setting. However, tuning tuner b either for $\Gamma_{out} = 0$ or for maximum power delivered to the load does not, in general, exactly satisfy either (12a) or (12b). Other complications with this method include inaccuracies due to nonideal source and load impedances [6]. The error in α from nonideal source impedance is not measurable using this method. The main problem with this technique, however, is that a tuner can have a value of α_0 for one tuning that is rather different from the value for the conjugate tuning.

Another method used for double-slug tuners is to conjugate tune one slug to tune out the other, then measure the attenuation of the tuner alone. This does not correctly account for losses in the line and connectors of the tuner beyond the two slugs.

The available gain of a matching network can be calculated from (2) or from (6), if the S-parameters are measured with high accuracy. The available gain of the matching network with ideal generator impedance α_0, requires only accurate $|S_{21}|$ and $|S_{22}|$. The accuracy in α_0 varies directly with that of $|S_{21}|^2$ and is very sensitive for large $|S_{22}|$. Fig. 4 shows the error in α_0 versus $|S_{22}|$ for various absolute errors in $|S_{22}|$ when there is no $|S_{21}|$ error. For typical GaAsFET's in the 2–12-GHz range, $|S_{22}|$ of a low-noise input-matching network ranges as high as 0.8 to effect minimum noise match.

S-parameter measurements with a magnitude accuracy of <0.01 are within the capability of computer-controlled, network-analyzer systems if multiple measurements are averaged [10], [11]. The system (ANA) used in the experiments is basically an HP 8409 system but is driven by PDP-11/70 minicomputer. A CW or narrow-band swept RF source was used to avoid "harmonic skipping" prob-

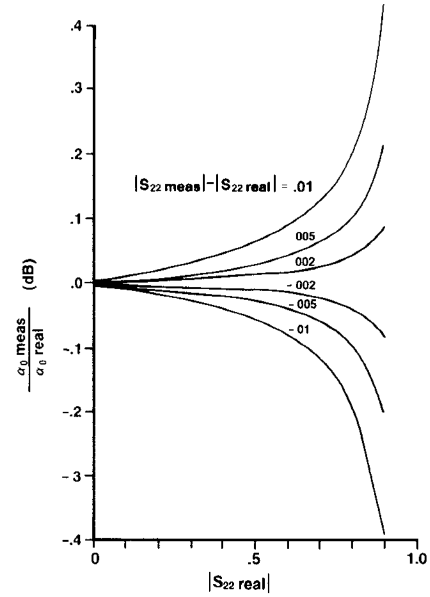

Fig. 4. Available gain error versus $|S_{22}|$ for various $|S_{22}|$ errors, when the available gain with an ideal source impedance is calculated from measured S-parameters. Subscript meas refers to the measured value, and subscript real refers to the actual value.

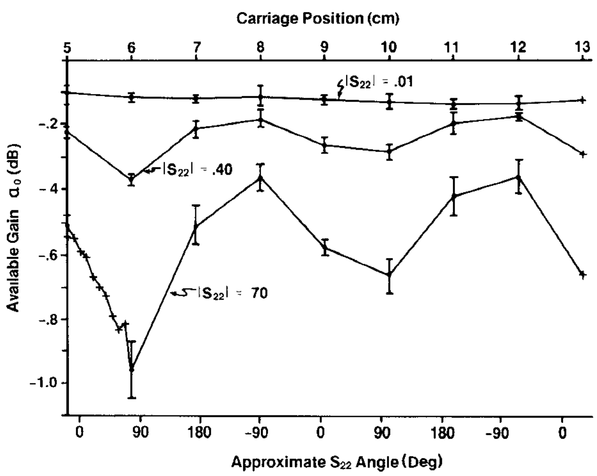

Fig. 5. Available gain with an ideal source impedance of a coaxial slide-screw tuner, measured on ANA at 4.0 GHz. + denotes three measurements averaged. ● denotes at least six measurements averaged.

lems, and full error modeling [12] was necessary to eliminate the effects of the source and load impedances. Repeatability was greatly improved by simply checking the calibration standards often between measurements. When the measured magnitude of any of the calibration standards had drifted more than 0.005, the system was recalibrated. The rms difference between the measured S_{21} and S_{12} of the matching circuits was typically 0.004 in magnitude and 0.6° in phase, which compares well with the expected reciprocity. For calculations of α, the average of the magnitudes of the measured S_{21} and S_{12} was used for $|S_{21}|$ in (6).

The available gain of a 2–18-GHz slide-screw tuner, Maury Microwave type 2640D, was measured on the ANA for various angle and magnitude settings at 4 GHz. Fig. 5 shows the results of these measurements. The error bars in this figure show the spread of α_0 from individual measurements (S_{21}, S_{22} pairs). As expected from Fig. 4, the spread is larger for larger $|S_{22}|$. This tuner is equipped with vernier scales for resetting a tuning condition. At 4 GHz, backlash was undetectable from carriage movement and was just detectable from stub micrometer positioning. Thus, settings were made by approaching a setting from one direction, as is done with a precision IF attenuator. As with most tuners, the loss is higher for higher $|S_{22}|$. Without appropriately correcting for the higher loss with higher $|S_{22}|$, the Γ_{min} apparent from tuning for minimum total noise figure has too small a magnitude. (GaAs MESFET's present more measurement difficulty than silicon bipolar transistors because a MESFET's $|\Gamma_{min}|$ is almost always much larger.)

The available gain was also a function of the S_{22} angle. After averaging numerous measurements, a half-wavelength (3.75-cm) periodicity in the available gain became apparent. This periodicity might be caused by radiation from the tuning element. It is this dependence on the S_{22} angle that makes back-to-back measurements of this tuner inaccurate. For example, if this tuner is tuned for $|S_{22}|=0.70$, where $\alpha_0=-0.9$ dB, an electrically identical tuner tuned for the same $|S_{22}|$ but conjugate angle will have $\alpha_0=-0.4$ dB. This phenomenon was confirmed in back-to-back measurements. The attenuation of the tuner pair was a strong function of S_{22} angle, and there was no way of telling which tuner had what loss. If there were no S_{22} angle dependence and if the different tuners had similar enough $|S_{21}|$ versus $|S_{22}|$ characteristics, then the back-to-back measurement with very good source and load matches would yield accurate available-gain data.

IV. Noise-Matching Circuit Measurements

Available-gain measurements were done on two microstrip matching networks for the input stage of a 3.7–4.2-GHz low-noise amplifier (LNA). Calibration standards that take into account the connectors on the microstrip circuits were used, and care was taken to shield the circuits in order to avoid radiation losses. Both circuits presented $|S_{22}|=0.75$ to a GaAsFET, but the minimum total noise figure (usually at midband) averaged 0.2 dB lower for circuit B than for circuit A in eight amplifiers built with each circuit from the same lot of FET's. Fig. 6 shows the available gain of circuits A and B as measured on the ANA. The difference in the available gain of circuits A and B agrees very well with the difference in noise performance. This available-gain measurement ascertained that circuit A was simply more lossy than circuit B, and that the difference in noise performance was not due to the circuit not presenting Γ_{min} to the FET or causing some type of spurious oscillation. Circuit A was built on alumina, while circuit B was built on teflon-fiberglass and had a different circuit topology. Circuit B was used for the input curcuit of an economical satellite earth station LNA having 120 K maximum effective input noise temperature over the 3.7- to 4.2-GHz band.

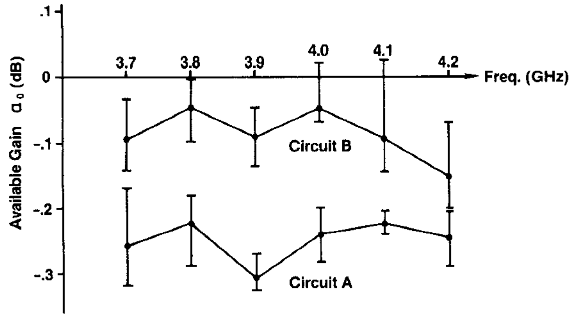

Fig. 6. Available gain with an ideal source impedance of two input matching circuits. Three measurements of circuit A were averaged, and seven measurements for three different tuning conditions of circuit B were averaged. Error bars show the spread of individual measurements.

Finally, the optimum noise figure of an FET (a selected NEC NE388) at 4 GHz was measured with two different networks. First, the FET was installed in circuit *B* and was biased and tuned for optimum noise figure at 4.0 GHz. The total noise figure of this amplifier at 4 GHz was 1.25 dB at the waveguide input. Subtraction of noise contributions from the input isolator, input matching network, and later stages implied a noise figure of 1.0 dB for the first-stage transistor. The FET was then removed and measured in the test setup of Fig. 1 using the tuner shown in Fig. 5 and the same input isolator and post-amplifier. When the input tuner and FET bias were adjusted for minimum total noise figure, the transistor's noise figure was 1.3 dB. The problem here is that the minimum total noise figure indicated does not correspond to the minimum first-stage noise figure for the following reasons. Since the later stages contribute to the total noise, the input tuning and FET biasing tend to optimize the gain of the first stage by compromising its noise figure. As noted above, the decrease in the tuner's available gain with increasing $|S_{22}|$ also tends to make the input tuning misleading.

Instead of randomly searching for the real minimum, the normal procedure is to measure the first-stage noise figure for about seven or more source admittances and then least-squares fit the data to (4) to find $F_{\min}$, $\Gamma_{\min}$, and r_n [13]. This procedure was performed with the tuner's corresponding measured available gain subtracted from the measured total noise figure for each tuning case. The $F_{\min}$ from the fitting program was 1.1 dB, and the calculated $|\Gamma_{\min}|$ was considerably larger than for the minimum total noise-figure tuning. Two other factors that probably contribute to the remaining 0.1-dB discrepancy are 1) the loss of an APC-7 coax-to-microstrip transition between the input tuner and the FET measurement plane, and 2) the transistor's bias may not have been exactly equal in both cases.

V. Conclusions

The noise-factor contribution of a passive two-port is equal to the inverse of its available gain and is given by (2). For low-loss passive circuits, the effect of non-Z_0 source impedance on the available gain is smaller with lower loss in the circuit. The back-to-back attenuation measurement of two tuners to determine the available gain of one of them assumes that the attenuation of the tuner pair is twice the available gain of either tuner. In practice, this can be a poor assumption.

Averaged measurements of a passive two-port on a computer-corrected network analyzer were successfully used to determine the available gain at 4 GHz of a slide-screw tuner and two matching circuits for a low-noise amplifier. Much higher accuracy is necessary as $|S_{22}|$ approaches unity, but data for $|S_{22}|=0.75$ agreed well with the noise performance of amplifiers using these networks. Measurement of the available gain of a matching network gives immediate insight into its best noise performance, whereas testing the circuit with its intended active device does not conclude whether extra noise is from circuit losses, $\Gamma_{\min}$ mismatch, spurious oscillations, nonoptimal biasing of the active device, or the device itself if it is not changeable.

The tuner problem is sometimes circumvented by selecting tuners with losses low enough to be ignored. Such a selection is not easy, depending on the accuracy desired, and usually results in limited tuning range and ease [14], [15]. The best double-slug coaxial tuners are less lossy than the slide-screw tuner measured here, but a slide-screw tuner has the advantage of almost independent magnitude and angle control. A major motivation for studying lossy noise-matching networks, however, is to show that the extra losses and source mismatch effects can be removed from the noise readings in a manner analogous to the removal of cable and adapter reflections by a computer-corrected network analyzer. Several decibels of loss can easily be removed as long as it is repeatable, as is done on a corrected network analyzer.

An automatic device-noise-parameter measurement system [16] can be assembled that electrically tunes the input, takes noise figure measurements, and quickly fits the data to find the noise parameters $F_{\min}$, r_n, and $\Gamma_{\min}$. A major problem with this approach is that the loss of an electrically tuned input tuner is much higher than that of mechanical tuners. This loss difference makes available-gain characterization of the tuner critically necessary. If the tuner has repeatable *S*-parameters, its available gain can be measured for each setting and then used to correct each noise figure measurement, as was done here for the slide-screw tuner example.

For low-noise amplifier development, what is needed is not a noise meter that measures the noise figure from a source impedance of approximately $50+j0\ \Omega$. Instead, the noise system should measure $F(\Gamma)$ for several Γ values and read out $F_{\min}$, $\Gamma_{\min}$, r_n, and $F(\Gamma)$ for any given Γ automatically over a frequency band. Such a system is necessary to collect sufficient noise data on active devices to define useful design windows. Measurement of an input-matching circuit cascaded with an active device on such a system would directly reveal the noise contribution of the matching circuit, how much figure improvement is possible from matching Γ_{min}, and what vector direction to tune to decrease $|\Gamma_{min}|$ at the input.

Acknowledgment

The author wishes to thank C. Hsieh, R. Q. Lane, P. Estabrook, and L. Lockwood for many helpful discussions.

References

[1] H. C. Okean and P. P. Lombardo, "Noise performance of M/W and MM-wave receivers," *Microwave J.*, vol. 16, no. 1, Jan. 1973.
[2] R. A. Pucel, D. J. Masse, and C. F. Krumm, "Noise performance of gallium-arsenide FET's," *IEEE J. Solid-State Circuits*, vol. SC-11, April 1976.
[3] W. W. Mumford and E. H. Scheibe, *Noise Performance Factors in Communications Systems*. Dedham, MA: Horizon House, 1968.
[4] "IRE standards on methods of measuring noise in linear twoports, 1959," *Proc. IRE*, vol. 48, pp. 60–68, Jan. 1960.
[5] C. K. S. Miller, W. C. Daywitt, and M. G. Arthur, "Noise standards, measurements, and receiver noise definitions," *Proc. IEEE*, vol. 55, June 1967.
[6] D. M. Kerns and R. W. Beatty, *Basic Theory of Waveguide Junctions and Introductory Microwave Network Analysis*. New York: Pergamon, 1967.
[7] T. Y. Otoshi, "The effect of mismatched components on microwave noise-temperature calibrations," *IEEE Trans. Microwave Theory Tech.*, vol. MTT-16, pp. 675–686, Sept. 1968.
[8] D. F. Wait, "Thermal noise from a passive linear multiport," *IEEE Trans. Microwave Theory Tech.*, vol. MTT-16, pp. 687–691, Sept. 1968.
[9] T. Mukaihata, "Applications and analysis of noise generation in N-cascaded mismatched two-port networks," *IEEE Trans. Microwave Theory Tech.*, vol. MTT-16, pp. 699–708, Sept. 1968.
[10] B. P. Hand, "Developing accuracy specifications for automatic network analyzer systems," *Hewlett-Packard J.*, pp. 16–19, Feb. 1970.
[11] E. F. Da Silva and M. K. McPhun, "Repeatability of computer-corrected network analyzer measurements of reflection coefficients," *Electron. Lett.*, vol. 14, no. 25, pp. 832–834, Dec. 1978.
[12] J. Fitzpatrick, "Error models for systems measurements," *Microwave J.*, pp. 63–66, May 1978.
[13] R. Q. Lane, "The determination of device noise parameters," *Proc. IEEE*, (Letters), vol. 57, pp. 1461–1462, Aug. 1969.
[14] G. Caruso and M. Sannino, "Computer-aided determination of microwave two-port noise parameters," *IEEE Trans. Microwave Theory Tech.*, vol. MTT-26, pp. 639–642, Sept. 1978.
[15] M. Mitama and H. Katoh, "An improved computational method for noise parameter measurement," *IEEE Trans. Microwave Theory Tech.*, vol. MTT-27, pp. 612–615, June 1979.
[16] R. Q. Lane, "A microwave noise and gain parameter test set," *ISSCC Dig. Tech. Pap.*, pp. 172–173, Feb. 1978.

Dependence of Electromagnetic Energy Deposition Upon Angle of Incidence for an Inhomogeneous Block Model of Man Under Plane-Wave Irradiation

MARK J. HAGMANN, MEMBER, IEEE, INDIRA CHATTERJEE, STUDENT MEMBER, IEEE, AND OM P. GANDHI, FELLOW, IEEE

***Abstract*—Whole-body and part-body energy deposition in a realistic inhomogeneous block model of man is presented as a function of angle of incidence for plane-wave irradiation for two cases: *E* arm-to-arm, with man in free space, *H* arm-to-arm, with man in free space, and also with man standing on a conducting plane. At the frequencies considered (27.12 and 77 MHz), the variation with angle is smooth and extrema occur at or near angles corresponding to the standard polarizations considered earlier by others. Part-body energy deposition and some of the fine structure in the angular dependence would not be seen with less realistic models of man.**

Manuscript received June 17, 1980; revised October 15, 1980. This work was supported in part by the National Institute of Environmental Health Sciences, Research Triangle Park, NC, under Grant 1RO1 ES 02304

The authors are with the Department of Electrical Engineering, University of Utah, Salt Lake City, UT 84112.

I. Introduction

THE increasing exposure of man-to-radio frequency energy has necessitated obtaining dosimetric information for use in the evaluation of possible biological effects.